1492 *Chem. Mater.* **2010,** *22,* 1492–1502
DOI:10.1021/cm902569g

CHEMISTRY OF MATERIALS
Article

Toward Submicrometer *c*-Oriented Nanoporous Films with Unidimensional Pore Network: AFI Film Morphology Control by Precursor Mixture Manipulation

Charitomeni M. Veziri,[†] Miguel Palomino,[‡] Georgios N. Karanikolos,*[,†] Avelino Corma,[‡] Nick K. Kanellopoulos,[†] and Michael Tsapatsis*[,§]

[†]*Institute of Physical Chemistry, Demokritos National Research Center, Athens 153 10, Greece,* [‡]*Instituto de Tecnologia Química (CSIC-UPV), Universidad Politecnica de Valencia, Avda de los Naranjos s/n, 46022 Valencia, Spain, and* [§]*Department of Chemical Engineering and Materials Science, University of Minnesota, 421 Washington Avenue SE, Minneapolis, Minnesota 55455*

Received August 24, 2009. Revised Manuscript Received December 18, 2009

c-Oriented, continuous $AlPO_4$-5 and CoAPO-5 films with an average thickness of as low as 500 nm were synthesized by seeded growth. Growth behavior was controlled by appropriate manipulation of the precursor mixture without altering hydrothermal temperature. Employing crystalline seeds and precrystallization of the precursor mixture under proper conditions yielded a controllable and uniform growth of prism-shaped oriented crystals over the entire substrate surface. Systematically altering the water content affected growth direction, which was continuously tuned between in-plane and *c*-out-of-plane. The AFI films synthesized by the present work being the first thin, oriented, and well-intergrown ones represent promising materials for fabricating high-flux, unidimensional-pore membranes, for hosting and organizing molecules and clusters, and for growing arrays of monodisperse and ultrathin nanostructures, such as carbon nanotubes, inside the AFI channels targeting highly efficient optoelectronic devices.

1. Introduction

Ordered framework materials exhibiting controlled crystal orientation, precise pore structure, stability, and activity offer great potential for a variety of applications such as separation membranes, shape-selective catalysts, adsorbents, ion exchangers, chemical sensors, and functional units in optical systems.[1−4] Aluminophosphate $AlPO_4$-5 (AFI structure) consists of one-dimensional, 12-membered ring channels with a 7.3 Å cross section that are arranged parallel to the *c*-axis of the crystal in a hexagonal lattice. Because of the unidimensional pore network, it has been suggested that transport through $AlPO_4$-5 membranes may exhibit orders of magnitude higher flux compared to multidimensional zeolites (e.g., MFI).[5,6] A variety of techniques have been developed for synthesis of AFI aluminophosphate (AlPO) molecular sieve deposits that exhibit preferred orientation, including alignment using electric field,[7,8] growth on premodified substrates[9] and under geometrical confinement,[5,10] laser ablation,[11] epitaxial growth,[12] and seeded growth,[13,14] yet the combination of orientation, small thickness (i.e., in the order of 1 μm), and continuity that could boost up film performance still remains unachievable.

For separation applications, intense research efforts currently focus on reducing the thickness of membranes in order to increase permeability while maintaining preferred orientation, without inducing film discontinuity or increasing defect densities that would compromise molecular selectivity.[2,13−15] In our previous work, oriented AFI films were developed by employing a modified seeded growth technique,[14,16] which improved control over film microstructure as it decoupled the nucleation from the growth processes by involving growth of predeposited particles (seeds). Exposing the seeds to secondary growth using a high H_2O:Al_2O_3 molar ratio favored *c*-out-of-plane growth yielding nonintergrown columnar

*Corresponding author e-mail: karanikolos@chem.demokritos.gr (G.N. K.), tsapatsi@cems.umn.edu (M.T.).

(1) Davis, M. E. *Nature* **2002**, *417*(6891), 813–821.
(2) Bein, T. *Chem. Mater.* **1996**, *8*(8), 1636–1653.
(3) Caro, J.; Noack, M.; Kolsch, P.; Schafer, R. *Microporous Mesoporous Mater.* **2000**, *38*(1), 3–24.
(4) Tsapatsis, M. *AIChE J.* **2002**, *48*(4), 654–660.
(5) Noack, M.; Kolsch, P.; Venzke, D.; Toussaint, P.; Caro, J. *Microporous Mater.* **1994**, *3*, 201–206.
(6) Kukla, V.; Kornatowski, J.; Demuth, D.; Girnus, I.; Pfeifer, H.; Rees, L. V. C.; Schunk, S.; Unger, K. K.; Kärger, J. *Science* **1996**, *272*(5262), 702–704.
(7) Caro, J.; Finger, G.; Kornatowski, J.; Richter-Mendau, J.; Werner, L.; Zibrowius, B. *Adv. Mater.* **1992**, *4*(4), 273–276.
(8) Lin, J. C.; Yates, M. Z.; Petkoska, A. T.; Jacobs, S. *Adv. Mater.* **2004**, *16*(21), 1944–1948.
(9) Feng, S.; Bein, T. *Science* **1994**, *265*(5180), 1839–1841.
(10) Wu, C. N.; Chao, K. J.; Tsai, T. G.; Chiou, Y. H.; Shih, H. C. *Adv. Mater.* **1996**, *8*(12), 1008–1012.
(11) Munoz, T.; Balkus, K. J. *Chem. Mater.* **1998**, *10*(12), 4114–4122.
(12) Xu, R.; Zhu, G. S.; Yin, X. J.; Wan, X.; Qiu, S. L. *Microporous Mesoporous Mater.* **2006**, *90*(1−3), 39–44.
(13) Lai, Z. P.; Bonilla, G.; Diaz, I.; Nery, J. G.; Sujaoti, K.; Amat, M. A.; Kokkoli, E.; Terasaki, O.; Thompson, R. W.; Tsapatsis, M.; Vlachos, D. G. *Science* **2003**, *300*(5618), 456–460.
(14) Karanikolos, G. N.; Wydra, J. W.; Stoeger, J. A.; García, H.; Corma, A.; Tsapatsis, M. *Chem. Mater.* **2007**, *19*(4), 792–797.
(15) Gouzinis, A.; Tsapatsis, M. *Chem. Mater.* **1998**, *10*(9), 2497–2504.
(16) Karanikolos, G. N.; García, H.; Corma, A.; Tsapatsis, M. *Microporous Mesoporous Mater.* **2008**, *115*(1−2), 11–22.

Published on Web 01/25/2010

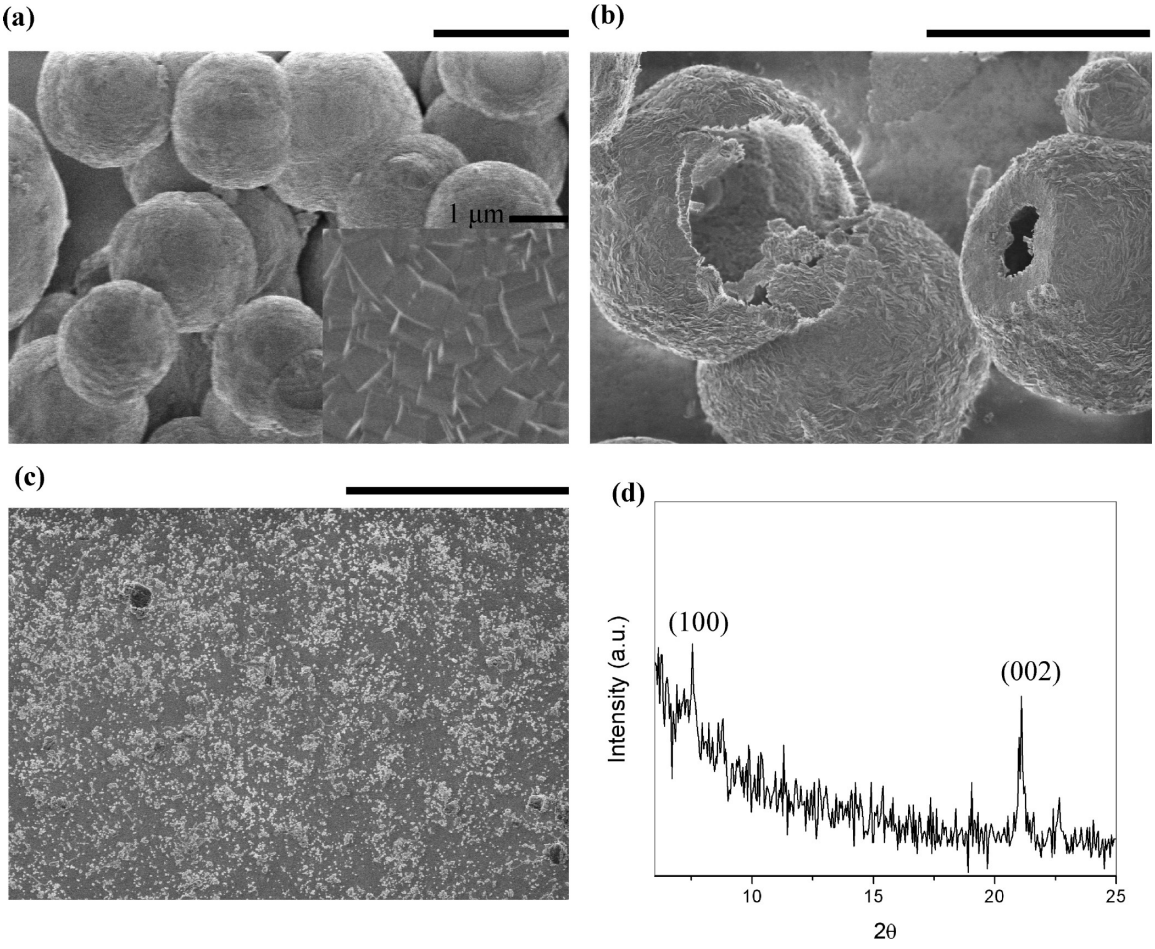

Figure 1. SEM image of CoAPO-5 powder used to produce seeds (a) before and (b) after treatment in HCl that was used to fracture the powder and form seed particles. (c) SEM image and (d) XRD pattern of a CoAPO-5 seed layer on silicon. The scale bars correspond to 50 μm.

crystals, which were subsequently interconnected by exposing them to a tertiary, in-plane growth under appropriate conditions. The outcome was well-intergrown, *c*-oriented $AlPO_4$-5 films with a thickness of several micrometers. On the other hand, using dense precursor mixtures favored in-plane growth and suppressed *c*-out-of-plane one thus offering potential for thickness reduction, nonetheless the high growth rate caused by the high nutrient concentration induced significant misorientation that compromised the quality of the resulting films. Here, we thoroughly investigate crucial parameters involved during preparation of the precursor mixture in an attempt to better control the growth behavior and achieve film thickness reduction while maintaining preferred orientation and continuity.

In parallel, the optimization study was expanded to cobalt-substituted $AlPO_4$-5 (CoAPO-5) films in order to dope the framework with transition metal, Brönsted acid catalytic sites. We are particularly interested in use of the developed catalytic microporous films as host−guest nanoreactor templates for synthesis of ultrathin and monodisperse carbon nanotube arrays. Ultrasmall single-walled carbon nanotube (SWCNTs) have attracted special attention due to their unique optical, electrical, mechanical, and electronic properties,[17−24] yet the extreme curvature and reactivity of these structures render their synthesis in well aligned, monodisperse populations a challenging issue.[25,26] Formation of monosized SWCNTs of the smallest diameter (4 Å) was recently templated in $AlPO_4$-5 powder,[17,27,28] via pyrolysis of the structure directing agent (SDA) inside the framework channels. To this extent, the small thickness, continuity, and orientation of the CoAPO-5 catalytic templates produced in the present work can trigger nanotube organization into parallel assemblies and direct oriented attachment on

(17) Wang, N.; Tang, Z. K.; Li, G. D.; Chen, J. S. *Nature* **2000**, *408* (6808), 50–51.
(18) Qin, L. C.; Zhao, X.; Hirahara, K.; Miyamoto, Y.; Ando, Y.; Iijima, S. *Nature* **2000**, *408*(6808), 50.
(19) Blase, X.; Benedict, L. X.; Shirley, E. L.; Louie, S. G. *Phys. Rev. Lett.* **1994**, *72*(12), 1878–1881.
(20) Hayashi, T.; Kim, Y. A.; Matoba, T.; Esaka, M.; Nishimura, K.; Tsukada, T.; Endo, M.; Dresselhaus, M. S. *Nano Lett.* **2003**, *3*(7), 887–889.
(21) Mao, Y. L.; Yan, X. H.; Xiao, Y.; Xiang, J.; Yang, Y. R.; Yu, H. L. *Phys. Rev. B* **2005**, *71*(3), 033404–4.
(22) Mohammadizadeh, M. R. *Phys. Status Solidi C* **2006**, *3*(9), 3126–3129.
(23) Mohammadizadeh, M. R. *Physica E* **2006**, *31*(1), 31–37.
(24) Peng, L. M.; Zhang, Z. L.; Xue, Z. Q.; Wu, Q. D.; Gu, Z. N.; Pettifor, D. G. *Phys. Rev. Lett.* **2000**, *85*(15), 3249–3252.
(25) Li, G. D.; Tang, Z. K.; Wang, N.; Chen, J. S. *Carbon* **2002**, *40*(6), 917–921.
(26) Wang, N.; Li, G. D.; Tang, Z. K. *Chem. Phys. Lett.* **2001**, *339*(1−2), 47–52.
(27) Tang, Z. K.; Sun, H. D.; Wang, J.; Chen, J.; Li, G. *Appl. Phys. Lett.* **1998**, *73*(16), 2287–2289.
(28) Chan, Y. F.; Peng, H. Y.; Tang, Z. K.; Wang, N. *Chem. Phys. Lett.* **2003**, *369*(5−6), 541–548.

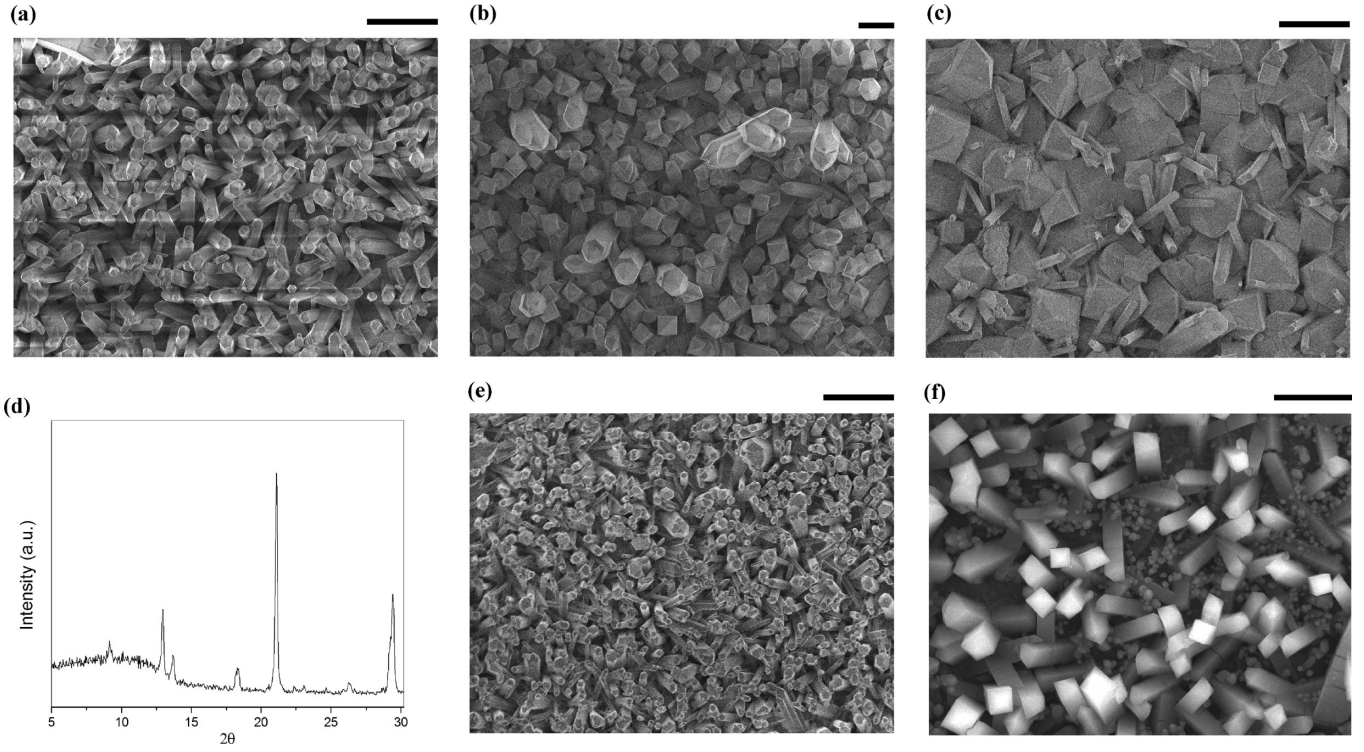

Figure 2. Sensitivity of film structure to temperature fluctuations during precursor mixture preparation. SEM images of films corresponding to a mixture preparation temperature of (a) < 10 °C, using an ice/water bath, (b) 25 °C, and (c) 25 °C with the exception that TEA was added at low temperature (~6 °C). The mixture molar composition was Al_2O_3:1.3P_2O_5:0.025CoO:1.2TEA:400H_2O and the secondary growth temperature and time were 150 °C and 10 h, respectively. (d) XRD pattern of a film corresponding to the high mixture preparation temperature indicating the formation of APC-type crystals. SEM images of films synthesized after precursor mixture preparation at room temperature (e) on a winter day and (f) on a summer day demonstrating transition of AFI- to APC-type structure, respectively. Scale bars correspond to 10 μm.

various supporting layers toward fabrication of highly efficient SWCNT-based devices.

2. Experimental Section

Film growth on silicon substrates took place hydrothermally at 150 °C in a conventional oven using a precursor mixture composition of Al_2O_3:1.3P_2O_5:(0.025CoO):1.2TEA:$x$$H_2O$. The procedure is reported in detail in our previous work[14,16] and in brief involves the following steps: (1) hydrolysis of aluminum isopropoxide in deionized water, (2) consecutive addition of phosphoric acid, triethylamine (TEA), and cobalt-II acetate tetrahydrate, (3) aging of the mixture for 12 h, and (4) hydrothermal reaction in a Teflon-lined autoclave. Prior to growth, the silicon substrates were cleaned, functionalized by 3-chloropropyltrimethoxysilane, and loaded with a monolayer of $AlPO_4$-5 or CoAPO-5 particles (seeds) by sonicating the functionalized substrates between two glass slides in a seeds-in-toluene suspension under humidity-free conditions.

Thermal pretreatment of the precursor mixture prior to growth was carried out at 150 °C. Thirty milliliters of the mixture after aging was introduced in an autoclave and inserted in the oven, which was preheated to the desired temperature. Following thermal treatment, the autoclave was removed and quenched in a cold water bath for 20 min, and the seeded substrate was inserted into the processed precursor mixtures at a position close to the upper surface of the liquid with the aid of a Teflon holder for secondary growth. Controlled-temperature precursor mixture preparation experiments were performed by mixing the precursor components using a water bath, where ice was periodically added to it in order to keep the temperature between 5 and 10 °C. The 12 h aging of the mixture was carried out under stirring in a refrigerator at a temperature of 5 °C. The molar composition in this set of experiments remained constant at Al_2O_3:1.3P_2O_5:0.025CoO:1.2TEA:400H_2O, while the growth temperature and time were set at 150 °C and 10 h, respectively.

Precursor mixture composition after thermal treatment and before introducing the seeded substrate was determined by inductively coupled plasma (ICP) of both the liquid and solid phases. The samples collected from the clear supernatant were diluted in MiliQ water, and the solids were dissolved in acid. The instrument used was a Varian 715-ES ICP-optical emission spectrometer. The TEA concentration in the supernatant was estimated through determining the C and N content in the recovered solid by elemental analysis using a Fissons EA-1108 elemental organic analyzer. Scanning electron microscopy (SEM) of the produced films was performed using a JEOL 6500 Field Emission Gun Scanning Electron Microscope (FEG-SEM) and a FEI Inspect SEM, while X-ray diffraction (XRD) was carried out using a Siemens D500 X-ray diffractometer in a $\theta/2\theta$ geometry, which is the technique of choice for preliminary analysis of preferred orientation given that in this way crystal planes that are parallel to the substrate are detected.

3. Results and Discussion

Before proceeding to secondary growth, experiments were performed in order to improve the crystalline quality of the seeds. Figure 1a is an SEM image of the CoAPO-5 powder used to produce seeds. The powder was formed by using a synthesis mixture molar composition of Al_2O_3: 1.3P_2O_5:0.025CoO:1.2TEA:100H_2O heated at 150 °C for 10 h. Initially, the powder consisted of large spherical particles with an average diameter of 50 μm that consisted

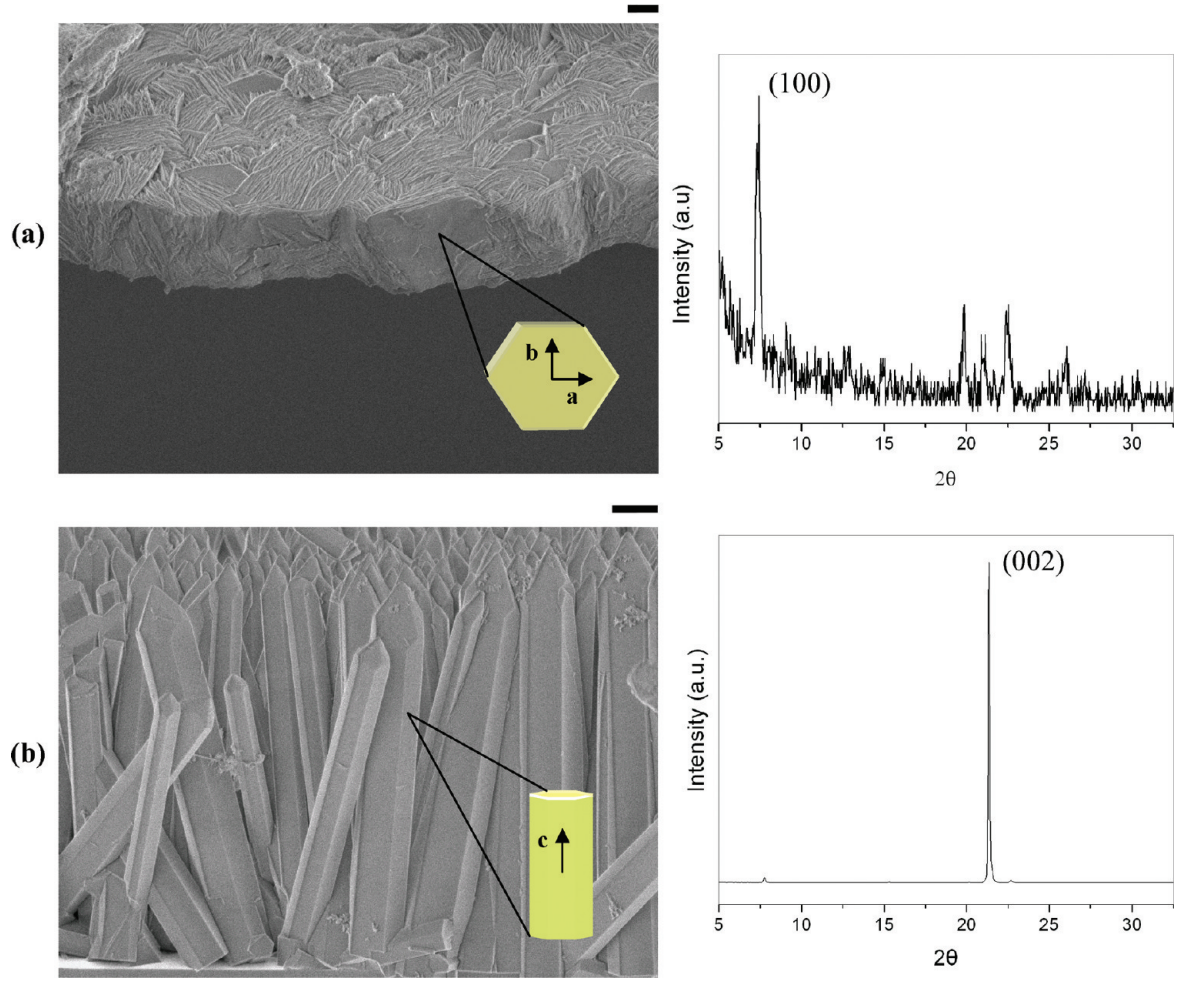

Figure 3. Morphology and orientation manipulation of $AlPO_4$-5 films grown at 150 °C by using a H_2O:Al_2O_3 molar ratio of (a) 100 and (b) 400. Scale bars correspond to 1 μm.

of flat-shaped intergrown CoAPO-5 crystals as well as from amorphous particles that were smaller in size and irregular in shape. The crystalline particles were deep-blue, a characteristic color of CoAPO-5,[29,30] and were isolated from the amorphous ones that were white, by allowing sedimentation by gravity in deionized water. The incorporation of Co^{2+} into the AFI framework under the present conditions has been confirmed by UV−vis Diffuse Reflectance Spectroscopy (DRS), shown in our previous set of data.[16] To produce CoAPO-5 particles for seeding, the crystals were exposed to 1 wt % hydrochloric acid (HCl) for 1 h or higher HCl concentration for shorter time (e.g., 10 wt % for 10 min). This treatment broke down the big spheres into small fractals as shown in Figure 1b. The particles produced after CoAPO-5 powder treatment in HCl were covalently attached onto the functionalized silicon substrates, as described in the Experimental Section. Figure 1c,d shows an SEM image and the corresponding XRD pattern of the deposited seed layer on silicon. The seed layer, though thin and discontinued, exhibits the main diffraction peaks of the AFI framework confirming the crystalline quality of the deposited particles.

3.1. Precursor Mixture Preparation Temperature. Growth experiments using different temperatures during preparation of the precursor mixture were first performed in order to investigate whether the mixture preparation temperature affects the quality of the resulting crystals. The molar composition in this set of experiments remained constant at Al_2O_3:1.3P_2O_5:0.025CoO:1.2TEA:400H_2O, which has been shown to yield columnar crystals,[14] while the growth temperature and time were set at 150 °C and 10 h, respectively. Interestingly, it was found that the mixture preparation temperature has a strong effect on the final crystal structure and can even change the crystalline phase of the resulting deposits. Figure 2a shows a typical columnar film of oriented hexagonal CoAPO-5 crystals corresponding to a mixture preparation temperature lower than 10 °C. Addition of the mixture components in this case was carried out in a water/ice bath at temperature between 5 and 10 °C, while the 12 h aging of the mixture was carried out under stirring in a refrigerator at a temperature of 5 °C. However, executing the mixture preparation at 25 °C yielded a non-AFI material, the morphology of which is shown in Figure 2b. We also repeated the experiment at 25 °C with the exception that the addition of TEA, being the most

(29) Fan, W. B.; Schoonheydt, R. A.; Weckhuysen, B. M. *Phys. Chem. Chem. Phys.* **2001**, *3*(15), 3240–3246.
(30) Shiralkar, V. P.; Saldarriaga, C. H.; Perez, J. O.; Clearfield, A.; Chen, M.; Anthony, R. G.; Donohue, J. A. *Zeolites* **1989**, *9*(6), 474–482.

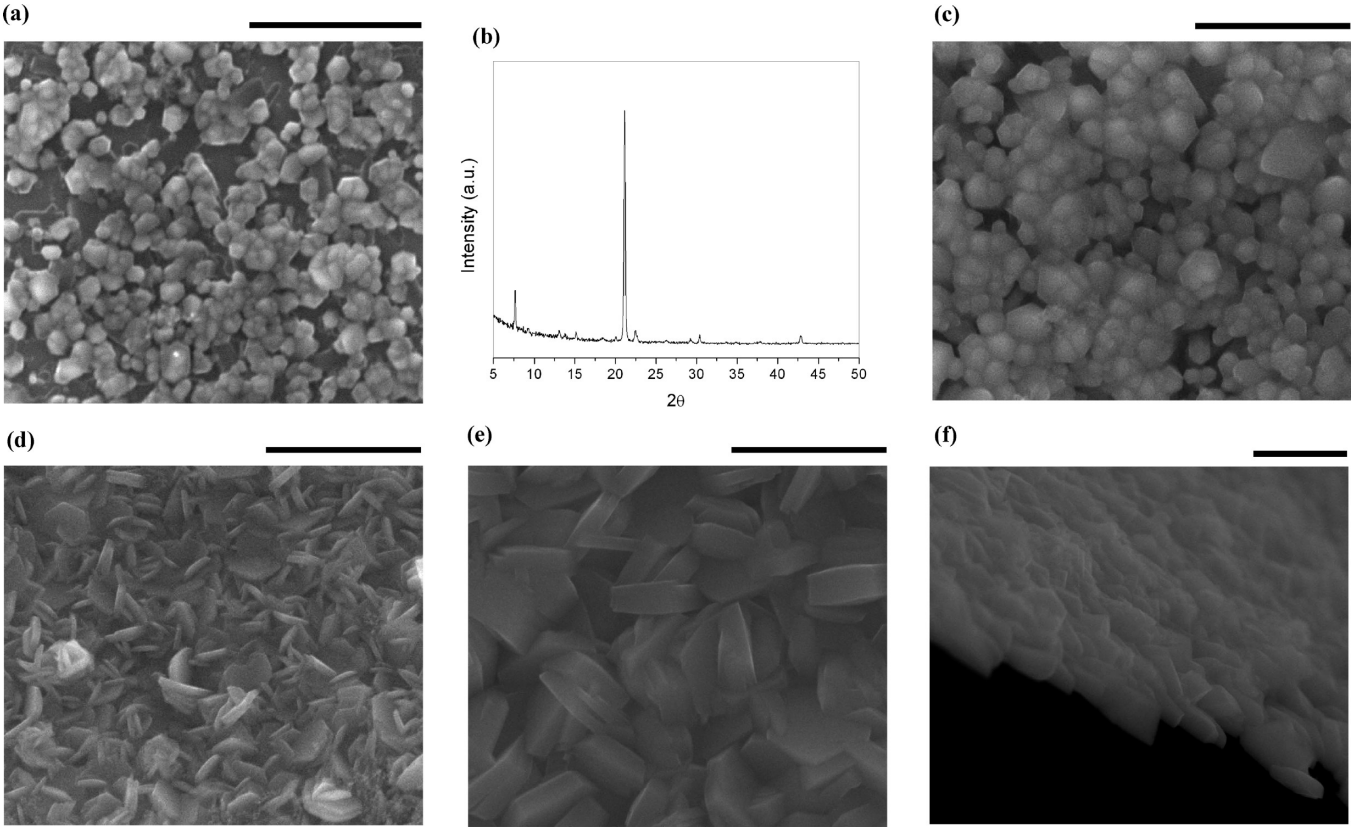

Figure 4. CoAPO-5 films grown by using a H_2O:Al_2O_3 molar ratio of 200. (a) SEM image and (b) XRD pattern of film corresponding to secondary growth duration of 4 h. (c) SEM image of film grown for 4.5 h. Intergrowth of misoriented grains taking place after a growth duration of (d) 5 h and (e), (f) 6 h. Scale bars correspond to 5 μm.

volatile compound, was carried out in an ice/water bath at ~6 °C. Once again, the resulting product consisted mainly by the non-AFI material, though the percentage of AFI grains was increased, as shown in Figure 2c. XRD characterization of the material corresponding to high temperature mixture preparation (Figure 2d) provided evidence of possible formation of CoAPO-H3 crystals, which exhibit the characteristic peaks of hydrated $AlPO_4$−C (APC structure).[31] $AlPO_4$−H3 consists of alternating $AlPO_4$ layers containing 8- and 4-oxygen membered rings ($8^2$4) and 6-oxygen membered rings (6^3), which are connected to construct a 3-dimensional network.[32] Previous studies have revealed that synthesis of this material is favored by excess in phosphate component[33] or by significant reduction of the organic template from the synthesis mixture,[34] conditions that can be easily attained in our case when mixture preparation takes place at high temperature, mainly due to amine evaporation. It is therefore necessary that the preparation of the reaction mixture is carried out under controlled conditions. To further support our findings, we compared two films obtained without any control of the preparation temperature (i.e., corresponding to mixtures prepared at room temperature), one on a winter and the other on a summer day. The room temperature between the two cases may vary by several degrees. Although the film synthesized on the winter day consisted of typical hexagonally shaped CoAPO-5 crystals (Figure 2e), the one synthesized on the summer day was dominated by the APC-type material (Figure 2f). Consequently, the observations of these experiments can be of particular importance to those working on growth of AFI and possibly other zeolite materials, as it can eliminate the critical but not enough-respected potential irreproducibility factor of film quality induced by temperature fluctuations during preparation of the precursor mixture.

3.2. Precursor Mixture Dilution. In our previous work,[14,16] we found that the water content in the precursor mixture affects drastically the morphology of the resulting AlPO crystals. Figure 3 compares $AlPO_4$-5 films produced by using the two H_2O:Al_2O_3 molar ratios used in that work. By using a concentrated reaction mixture (H_2O:Al_2O_3 = 100), fast growth along the a-, b-axis of the crystal, i.e. perpendicular to AFI channels, is favored producing thin crystals, which are well-intergrown but are oriented with their channels parallel to the support, as the SEM image and corresponding XRD pattern in Figure 3a depict. On the other hand, using a dilute reaction mixture (Figure 3b, H_2O:Al_2O_3 = 400) and keeping the molar ratio with respect to Al_2O_3 of the rest of the components, as well as the reaction temperature constant, i.e. Al_2O_3:1.3P_2O_5:1.2TEA and 150 °C respectively,

(31) Canesson, L.; Arcon, I.; Caldarelli, S.; Tuel, A. *Microporous Mesoporous Mater*. **1998**, *26*(1−3), 117–131.
(32) Kunii, K.; Narahara, K.; Yamanaka, S. *Microporous Mesoporous Mater*. **2001**, *50*(2−3), 181–185.
(33) D'Yvoire, F. *Bull. Soc. Chim. Fr*. **1961**, 1762–1776.
(34) Kunii, K.; Narahara, K.; Yamanaka, S. *Microporous Mesoporous Mater*. **2002**, *52*(3), 159–167.

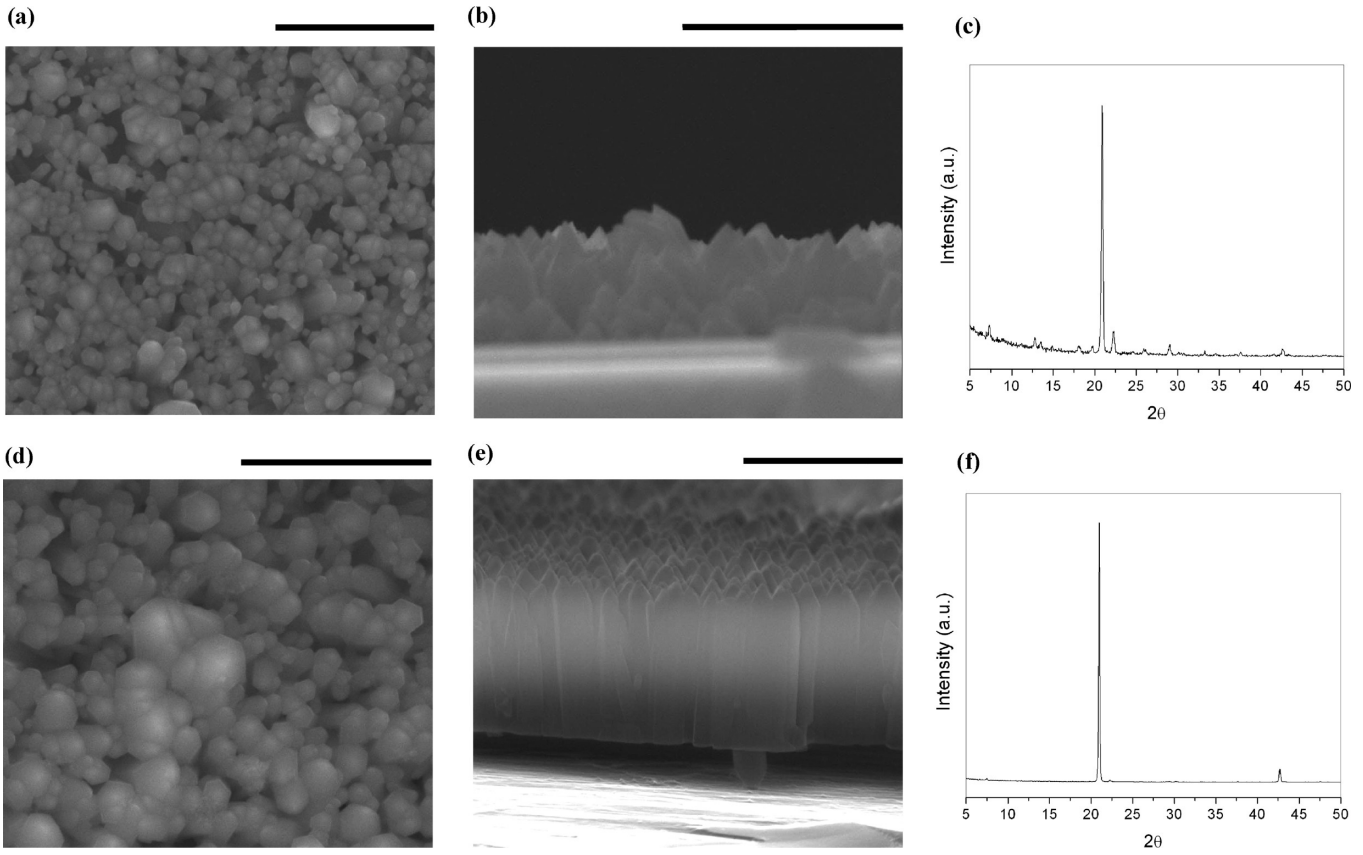

Figure 5. CoAPO-5 films grown by using a H_2O:Al_2O_3 molar ratio of 300 after a secondary growth of (a), (b), (c) 4 h, (d) 5 h, and (e), (f) 6 h. Misoriented intergrowth is not observed even after extended growth duration. Scale bars correspond to 5 μm.

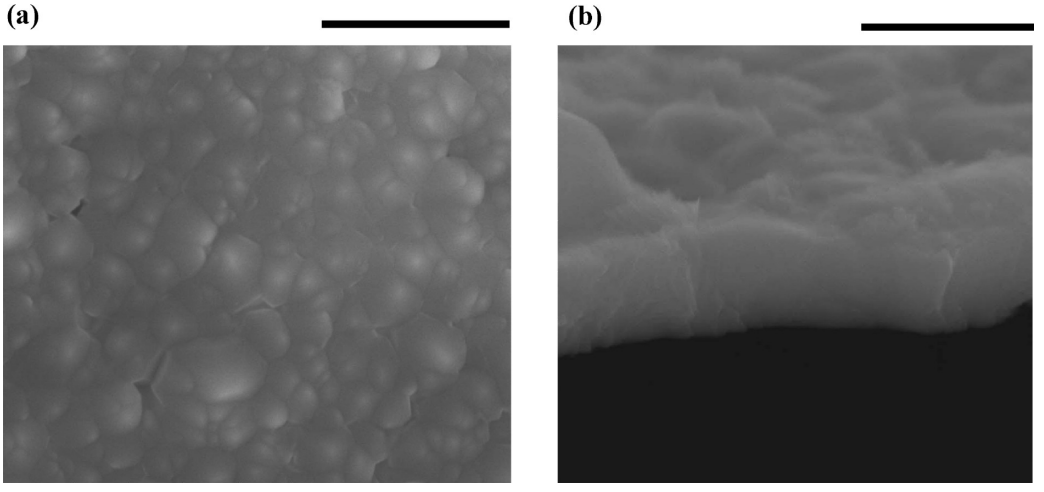

Figure 6. Tertiary, in-plane growth of (a) the film corresponding to a H_2O:Al_2O_3 molar ratio of 300 and 4 h secondary growth (shown in Figure 5a) and (b) the film corresponding to a H_2O:Al_2O_3 molar ratio of 200 and 4.5 h secondary growth (shown in Figure 4c). The tertiary growth duration was 2 h 20 min and 3 h, respectively. Scale bars correspond to 5 μm.

growth along the *c*-axis was favored yielding columnar crystals, which are well-oriented but form a relatively thick and discontinuous film. *c*-Orientation is confirmed by XRD analysis (Figure 3b, right), which shows that the intensity ratio of the (100):(002) reflections that expresses the ratio of channels parallel versus channels perpendicular to support is minimal compared to that of a pattern of AFI powder that does not exhibit any preferred orientation. These findings motivated us to further study the effect of water content to the quality of the final film by systematically varying mixture dilution using intermediate H_2O:Al_2O_3 molar ratios, in an attempt to reduce film thickness but without sacrificing orientation and continuity.

Figure 4 corresponds to a H_2O:Al_2O_3 molar ratio of 200. It is evident that even for the early stages of growth (Figure 4a, 4 h) misorientation is considerably suppressed compared to the samples corresponding to the H_2O:Al_2O_3 molar ratio of 100 (Figure 3a), as also confirmed by the corresponding XRD pattern shown in Figure 4b. Increasing growth time (Figure 4c, 4.5 h), the film continues to

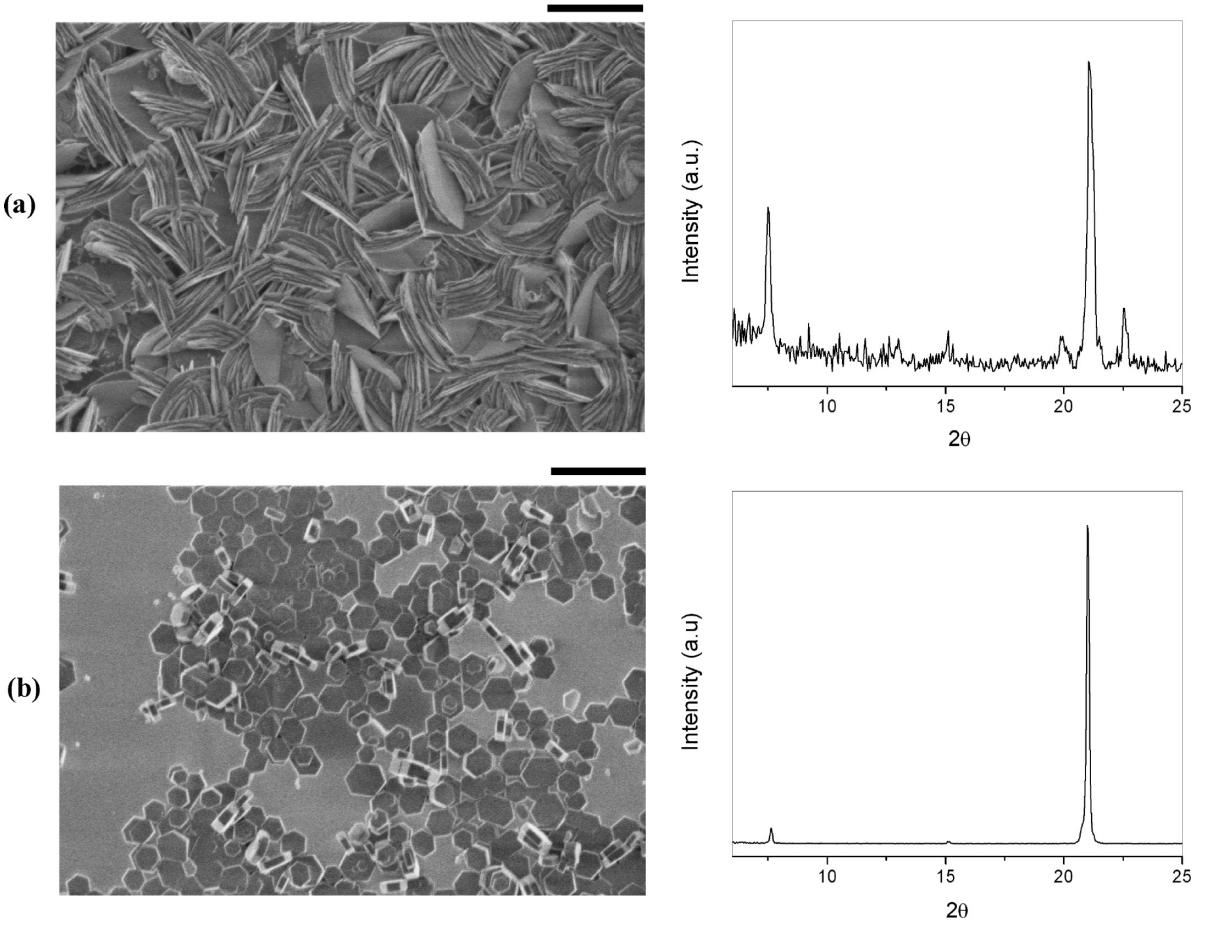

Figure 7. Crystal morphology manipulation by varying the thermal pretreatment duration of the reaction mixture. SEM (left) and corresponding XRD (right) images of CoAPO-5 films obtained after a thermal pretreatment and secondary growth time of (a) 10 h, 1 h 30 min, and (b) 24 h, 2 h, respectively. Scale bars correspond to 2 μm.

grow following the preferred orientation, while concurrent in-plane growth gradually fills the gaps between the oriented grains. Increasing reaction time further however (Figure 4d, 5 h), despite the fact that the film is now well-intergrown, misoriented crystals are formed on the top of the initial oriented ones. These crystals increase in number and size by increasing growth time (Figure 4e, 6 h), yet the overall film thickness remains small, i.e. at approximately 2 μm, as shown by the side-view SEM image of Figure 4f.

To further suppress growth of misoriented grains, we increased the H_2O:Al_2O_3 molar ratio to 300 (Figure 5). For a reaction time of 4 h (Figure 5a, b), hexagonal crystals are grown perpendicular to support forming a film with an average thickness of 2 μm, which exhibits preferred orientation, as indicated by the XRD pattern in Figure 5c. For higher reaction times, crystals continue to grow along the *c*-out-of-plane direction (Figure 5d, 5 h), while there is no evidence of formation of misoriented grains, as also shown in the cross-section SEM image of Figure 5e and the respective XRD pattern (Figure 5f), which correspond to a reaction time of 6 h.

In order to completely fill the gaps of the thinner films produced using the intermediate H_2O:Al_2O_3 molar ratios described above, we executed tertiary growth using concentrated precursor mixtures (H_2O:Al_2O_3 = 100) in order to enable in-plane, oriented intergrowth of the secondary crystals. Figure 6a shows the film corresponding to a H_2O:Al_2O_3 molar ratio of 300 and 4 h secondary growth, which is depicted in Figure 5a,b,c, after it has undergone a tertiary growth treatment for 2 h 20 min at 150 °C. Comparing Figures 5a and 6a, we realize that the intergrain gaps have been closed offering film continuity without evidence of misorientation. The cross-section SEM image in Figure 6b, which corresponds to a 3 h tertiary growth of the film shown in Figure 4c (H_2O:Al_2O_3 = 200, 4.5 h secondary growth), demonstrates that tertiary growth does not increase film thickness (which remains at about 2.5 μm), owing to the in-plane, oriented intergrowth that takes place under the present conditions.

3.3. Precursor Mixture Thermal Pretreatment. To provide an additional optimization parameter toward finer control over film growth, the precursor mixture was thermally treated before secondary growth using different treatment durations, in an attempt to alter its activity by causing a first crystallization before introducing the seeded substrate and study the effect on the morphology of the resulting AlPO films. This treatment took place in an autoclave at the same temperature as the one used for film growth (150 °C), using a mixture molar composition of Al_2O_3:1.3P_2O_5:0.025CoO:1.2TEA:100H_2O. Under

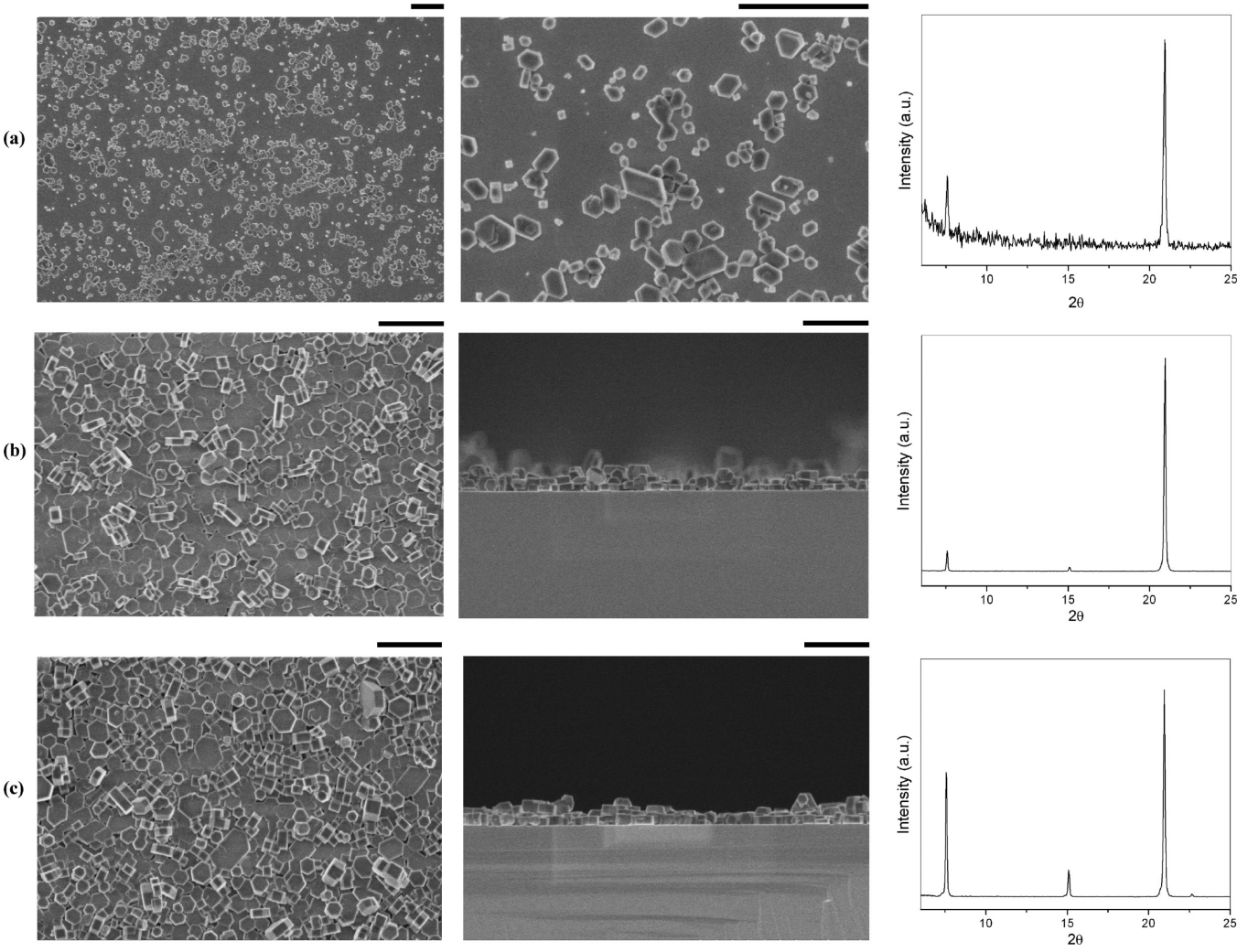

Figure 8. SEM images and corresponding XRD patterns of CoAPO-5 films obtained after a 30 h thermal pretreatment using a secondary growth duration of (a) 2 h, (b) 2 h 30 min, and (c) 3 h. Scale bars correspond to 2 μm.

these conditions, crystallization has been shown to occur for reaction duration as short as 10 h (Figure 1a), thus longer reaction times have been selected in the precrystallization experiments performed, so as to manipulate the concentration of the available nutrients before secondary growth. The duration of the pretreatment thus the extent of the first crystallization was found to strongly affect the characteristics of the resulting film. Figure 7 shows SEM images and corresponding XRD patterns of films obtained after different thermal pretreatment times. A 10 h pretreatment (Figure 7a) yielded flakelike crystals due to fast growth perpendicular to the AFI channels caused by the relatively high concentration of the nutrients that are still available in the pretreated mixture. In addition, fast growth resulted in high intergrowth of misoriented grains which compromised film orientation. By increasing pretreatment duration to 24 h, the growth rate was significantly reduced, and growth along the *c*-direction was favored yielding hexagonally shaped yet thin crystals, while the degree of misorientation was suppressed, as the SEM image and XRD pattern in Figure 7b reveal. However, the growth is still too fast to allow complete coverage without misoriented growth to occur.

Figure 8 shows CoAPO-5 films obtained using a precrystallization time of 30 h. For a growth time of 2 h (Figure 8a), seed growth has been initiated, and crystals with an average width of 500 nm and thickness of 200 nm having a broad size distribution are apparent. As SEM images reveal, the crystals, although small, tend to acquire the hexagonal shape and are grown with their channels perpendicular to substrate (flat side up) following the orientation of the seeds, while a few misoriented grains (channels parallel to substrate) can also be found that are probably generated by growth of the small portion of seeds that are misoriented. *c*-Orientation is also confirmed by XRD (Figure 8a right), which shows a very small intensity ratio of the (100):(002) reflections. At 2 h 30 min (Figure 8b), crystals have been well-intergrown forming a film with an average thickness of approximately 500 nm. Cross-sectional SEM analysis demonstrates that a monolayer of crystals is preferentially grown, while a second layer appears in some parts of the support. The presence of a small number of misoriented crystals that appear to have intergrown on the original oriented ones is also evident. The XRD pattern, however, confirms that the number of these misoriented

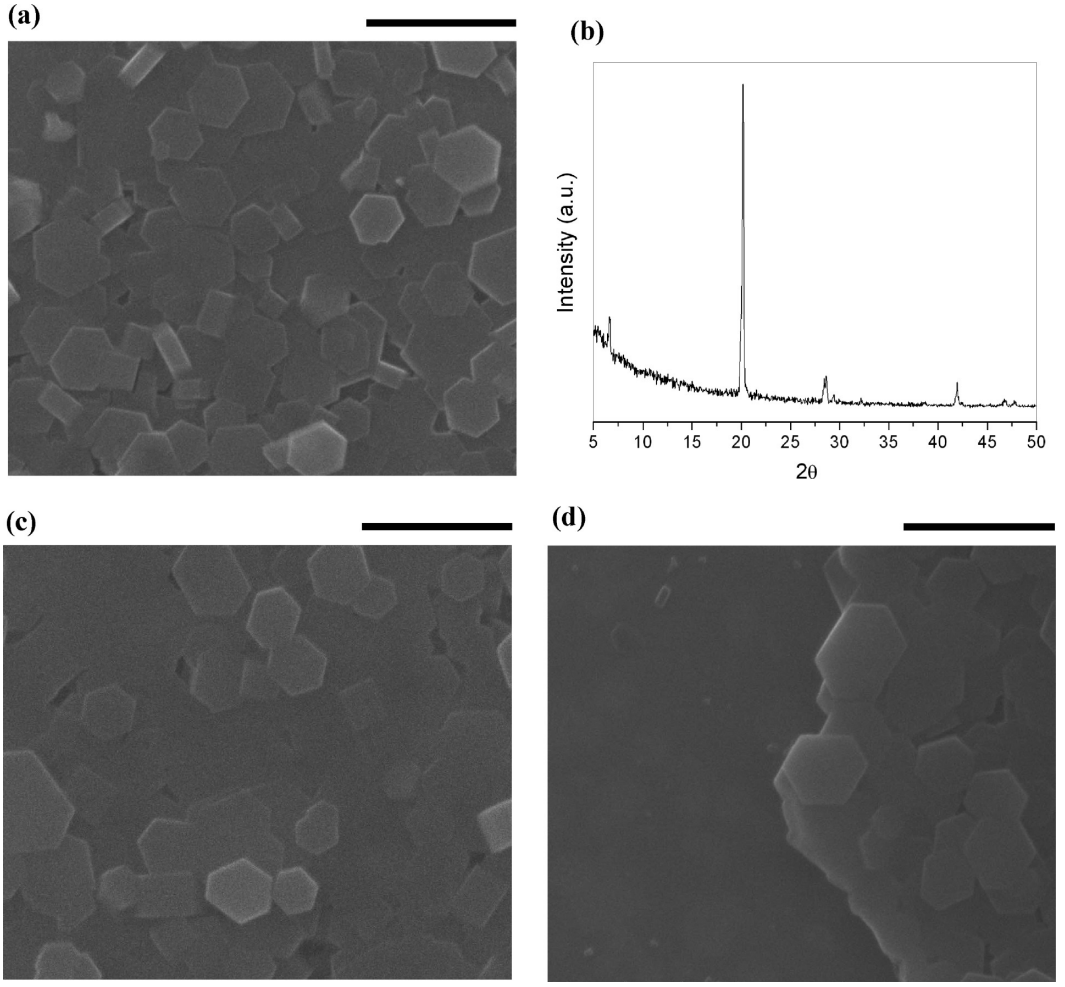

Figure 9. CoAPO-5 films after a 48 h precursor mixture thermal pretreatment. The secondary growth time was (a), (b) 6 h, and (c), (d) 7 h. Scale bars correspond to 2 μm.

grains is minimal compared to the oriented ones, as shown by the strong enhancement of the reflection that corresponds to the (002) plane. For higher secondary growth times (3 h), film thickness increases and formation of misoriented crystals is augmented, as indicated by the SEM image and corresponding XRD pattern in Figure 8c.

In order to further enhance crystal intergrowth and minimize misorientation, we increased thermal pretreatment duration, which was followed by an analogous increase in secondary growth time. Figure 9 corresponds to a pretreatment time of 48 h. The SEM image in Figure 9a indicates that the synthesized hexagonal crystals after a 6 h growth are well intergrown forming a continuous film, which exhibits preferred orientation as confirmed by the corresponding XRD pattern (Figure 9b). Increasing growth time to 7 h without changing pretreatment duration (Figure 9c) further improved film intergrowth without formation of misoriented grains to have taken place. Under these conditions therefore, film continuity and orientation have been enhanced, while a small film thickness (i.e., in the order of 1 μm) has been achieved, as indicated by the SEM image in Figure 9d. Experiments continued using even longer pretreatment (i.e., 60 h) and growth, but in both cases either it was difficult to achieve a complete coverage or crystals tended to grow following a rather random orientation. An intermediate pretreatment duration therefore, combined with appropriate secondary growth time, was optimal in order to obtain a continuous and thin film while maintaining *c*-out-of-plane orientation.

To correlate the morphology of the resulting films with the composition of the pretreated precursor mixtures, the supernatants (i.e., the portion that would be in contact with the growing film) after different precrystallization times were analyzed. The Al, P, Co, and TEA concentrations after 24 h and 48 h precrystallization are shown in Figure 10a and compared with the starting gel. Long precrystallization (24 h and 48 h) of the initially dense reaction mixtures caused considerable reduction of the amount of nutrients, which were consumed for the formation of the crystalline powder, thus increasing the dilution of the remaining nutrients, a fact that is visually confirmed through the transition between milky to clear supernatants. The alterations in species content induced by precrystallization affected the morphology of the crystalline grains and the characteristics of the obtained film.

From the composition analysis of the supernatant, it is apparent that a considerable drop in Al and P concentration takes place during the first 24 h, which becomes much

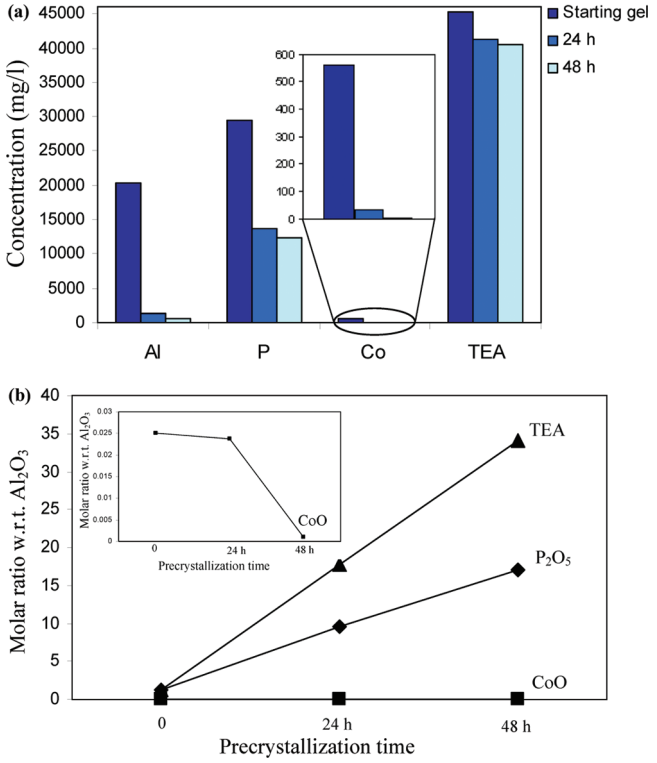

Figure 10. Characterization of the precrystallized precursors. (a) Al, P, Co, and TEA concentration determined by ICP and elemental analysis before and after precrystallization for 24 h and 48 h. (b) Evolution of molar ratios with respect to Al_2O_3 with precrystallization time.

less significant for longer reaction times. In addition, most of Co is removed from the supernatant to precipitated solid during the first 24 h processing. Taking into account ICP evidence from the recovered precipitate, it is estimated that approximately 95% and 99.8% of the initial Co amount after 24 h and 48 h treatment, respectively, is in the solid. In contrast, a relatively small consumption of TEA is observed in all treatment durations tested. The disproportional reduction of Al versus P in the supernatant and the low TEA consumption compared to that expected for highly crystalline CoAPO-5 are attributed to the formation of a significant amount of amorphous material that is precipitated together with the crystals during the precrystallization treatment, as confirmed by SEM and XRD analysis of the recovered solid (data not shown). Indeed, based on the fact that the framework unit cell consists of 24 T atoms (T = Al, P, Co), if we assume that all the amount of T atoms measured in the solid belongs to crystalline material, the number of TEA molecules per unit cell after 24 h precrystallization is calculated to be 0.8, which is lower than that reported for crystalline CoAPO-5 (1.27).[35] However, the presence of amorphous material justifies the low value, giving that a significant portion of the T atoms do not actually belong to the crystals but to the amorphous material. For 48 h precrystallization, the number of TEA molecules per unit cell increases to ~1, mainly due to suppression of the amount of amorphous phase in relation to the crystalline one caused by longer reaction, which increases the portion of T atoms that belong to the crystals. The evolution of the precursor molar ratio in the supernatant with precrystallization time, which is shown in Figure 10b, indicates that the P_2O_5 and TEA molar ratios with respect to Al_2O_3 increase almost linearly with time, reaching a value of approximately 15 and 35, respectively, after 48 h of reaction. These are considerably higher than the corresponding molar ratios for the starting gel, which are 1.3 and 1.2. At the same time, the $CoO:Al_2O_3$ molar ratio decreases with precrystallization time and Co is almost exhausted after 48 h, as shown in the insets of Figure 10a,b.

Considering only the high water content of the resulting liquids after precrystallization that are subsequently used for secondary growth, one would expect to observe growth behavior similar to that observed using precursor mixtures with high $H_2O:Al_2O_3$ molar ratio, i.e. thick films consisting of long columnar crystals (Figure 3b). However, the high TEA and P_2O_5 molar ratios in the precrystallized mixtures, as shown by the data of Figure 10b, apparently counteract this effect and suppress the length of the columnar crystals. This effect is in qualitative agreement to powder experiments investigating $AlPO_4$-5 crystal morphology for different precursor compositions, which have shown that increasing the amine molar ratio resulted in formation of smaller crystals, while an analogous behavior was also observed when the P_2O_5 content was increased.[36] In addition, given that the presence of Co favors formation of longer crystals compared to nonsubstituted $AlPO_4$-5,[16] the reduction in Co content that was observed in the precrystallized precursors also appears to contribute to the formation of thinner films. Therefore, the hexagonal shape of the crystals and the slow nucleation/growth were achieved due to nutrient dilution induced by the precrystallization (in contrast to dense starting mixtures that result in formation of flake-like crystals (Figure 3a)), yet the balance between dilution and nutrient molar ratios of the resulting precursors kept the crystal size small, thus producing films that combine preferred orientation with continuity and small thickness. Of course more subtle effects associated with speciation details that cannot be revealed by simple elemental analysis cannot be excluded as contributors to the observed microstructures.

Interestingly, carrying out long enough precrystallization considerably suppresses the tendency to misoriented growth even from the early stages of film formation. In support of this, Figure 11a,b shows SEM images of films grown after a 2 h and a 48 h pretreatment, respectively, where the reaction has been stopped before considerable crystal intergrowth has been attained. A comparison between the two images demonstrates that when a short pretreatment is used, heavy intergrowth takes place from the beginning of film formation. In contrast, only a few misoriented grains are observed in the SEM image

(35) Montes, C.; Davis, M. E.; Murray, B.; Narayana, M. *J. Phys. Chem.* **1990**, *94*(16), 6425–6430.

(36) Finger, G.; Richtermendau, J.; Bulow, M.; Kornatowski, J. *Zeolites* **1991**, *11*(5), 443–448.

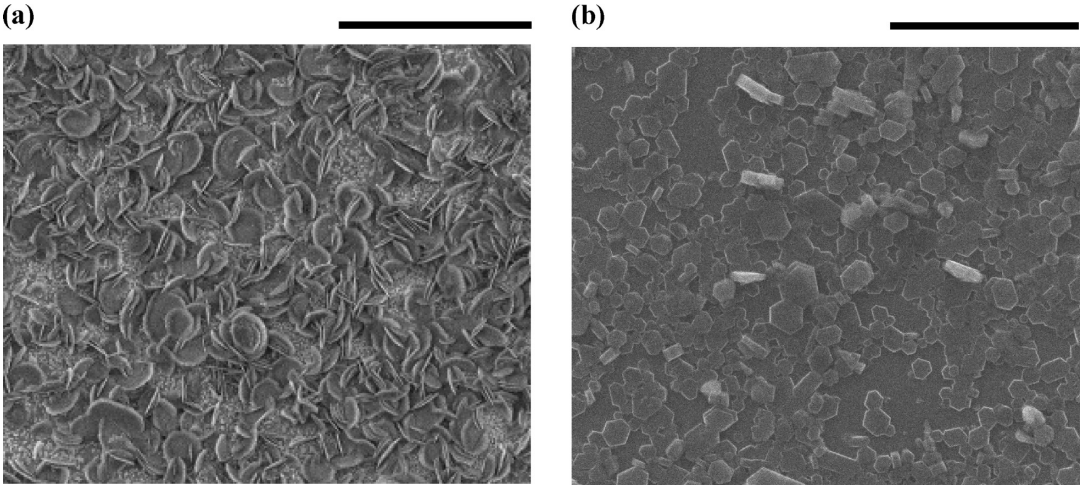

Figure 11. Early stages of film growth after a precursor mixture thermal pretreatment of (a) 2 h and (b) 48 h. Extended pretreatment favors oriented growth even from the early stages of film formation. Scale bars correspond to 5 μm.

corresponding to a pretreatment time of 48 h (Figure 11b), indicating that the film in this case starts growing following the preferred orientation and ultimately evolves into a continuous one maintaining the preferred orientation (Figure 9). Conclusively, the absence of a gradual transition from random orientation to *c*-preferred-orientation indicates that the formation of these thin and oriented films is not based upon competitive growth, which would evolve through domination of oriented crystals at the expanse of outgrown misoriented ones, but rather proceeds through oriented intergrowth of originally oriented grains.

4. Conclusions

The growth behavior of $AlPO_4$-5 and metal-substituted $AlPO_4$-5 films was controlled by appropriate manipulation of parameters involved during the pregrowth stage. Using a constant mixture composition and hydrothermal temperature, we focused on processes related to precursor mixture preparation in an attempt to affect growth. Systematic manipulation of the water content, thermal pretreatment, and preparation temperature of the mixture resulted in a variation of film morphologies, while under optimal conditions films that exhibited *c*-orientation, continuity, and small thickness were obtained. Using intermediate dilutions of the precursor mixture (H_2O:Al_2O_3 molar ratio of 200 and 300) suppressed misorientation significantly and reduced film thickness down to approximately 2 μm after a secondary growth duration of 4 h at 150 °C. Without increasing film thickness or inducing considerable misoriented intergrowth, tertiary, in-plane, and oriented growth using concentrated mixtures (H_2O:Al_2O_3 molar ratio of 100) closed the intercrystalline gaps yielding continuous films. Long thermal pretreatment (precrystallization) of concentrated precursor mixtures at 150 °C balanced precursor dilution with appropriate nutrient molar ratios yielding flat hexagonal crystals that were grown with their channels perpendicular to support. As a result, formation of oriented films with an average thickness of 500 nm was realized, after a pretreatment of 30 h and a secondary growth of 2 h 30 min. 48 h thermal pretreatment followed by a 7 h growth further enhanced crystal intergrowth while maintaining preferred orientation and yielded films with a thickness of approximately 1 μm. The AFI films prepared here, being the first thin, oriented, and continuous ones, represent an important step forward toward realization of high quality unidimensional-channel films that can open up new prospects in such areas as high-flux membranes, molecular hosting and organization, and templated growth of nanostructures inside the oriented pores, with numerous potential applications ranging from advanced separations to highly efficient optoelectronics.

Acknowledgment. We thank I. Zafiropoulou for assistance with XRD characterization. Support by the Initiative for Renewable Energy and the Environment (IREE) and the American Chemical Society (PRF) is greatly appreciated. Support by PROMETEO and the European network of excellence INSIDE PORES is also acknowledged. G.N.K. acknowledges support by the European Community, Marie Curie International Reintegration Grant (FP7, grant agreement no. 210947). M.P. thanks CSIC for a JAE doctoral fellowship.